
Localized Turbulent Structures in Long Pipe Flow with Minimal Set of Reflectional Symmetry

S. Altmeyer

Castelldefels School of Telecom and Aerospace Engineering (EETAC), Universitat Politècnica de Catalunya,
08860 Barcelona, Spain

e-mail: sebastian.andreas.altmeyer@upc.edu

Received September 6, 2021; revised October 4, 2021; accepted October 21, 2021

Abstract—The laminar-turbulent boundary (edge) separates trajectories approaching a turbulent attractor from those approaching a laminar one, at least for a finite time. To investigate the flow dynamics on the edge we carried out direct numerical simulations of transitional pipe flow (here at Reynolds number $Re \in [2200, 2800]$) in a long computational domain. The studied solution has the form of a structure localized in space and traveling downstream. Its qualitative characteristics are similar to the turbulent puffs observed experimentally in the transitional Reynolds number regime. The dynamics within the saddle region of the phase space on the separatrix (hyper-surface in pipe flow) appears to be chaotic. Here, we report such localized solutions on the edge/separatrix for pipe flow and investigate their correlation to turbulent puffs using a minimal set of (artificial) restrictions to the states, i.e., the mirror symmetry, and investigate the resulting flow behavior in this subspace. In contrast to higher symmetry restricted solutions, here detected solutions on the separatrix turn out to be quite as complex as the full state solutions. Worth emphasizing that any solutions found in the subspace are also solutions of the full space and therefore represent physical (symmetric) flow states.

Keywords: Navier–Stokes equations, turbulent puffs, edge states, computational fluid dynamics

DOI: 10.1134/S001546282202001X

Turbulence is the rule rather than an exception in nature but our understanding of turbulence is limited to statistic quantities. Thus the general aim is to disentangle the dynamics close to the onset of turbulence. In particular, transition to turbulence in pipe flows is a still remaining open problem of stability theory. Pipe flow, the fluid flow through an infinite long pipe of circular cross-section, i.e., the Hagen–Poiseuille flow, is believed to be always stable with respect to infinitesimal perturbations [1] but it is known to become turbulent in practice [2, 3].

The characteristic parameter to identify the flow is the Reynolds number, defined as $Re = UD/\nu$, where U is the mean velocity of the flow, D is the pipe diameter, and ν is the kinematic viscosity. Typically, instabilities in pipe flow are observed for Re greater than 1750 [3, 4]. Within the range $Re \in [1750, 2700]$ perturbations can trigger transition to intermittent turbulent spots usually called *puffs*, which coexist with the laminar Hagen–Poiseuille flow [2, 5]. At Re up to 2250 turbulence appears to be localized in the form of puffs and, as a result, upstream and downstream front speeds of these structures are identical. Increasing Re results in decreasing front speeds. Wignanski et al. [6] introduced the notation of “an equilibrium puff” (for $2100 < Re < 2300$) at which parameters (dimensions and Re fixed) do not change in the course of its motion in the pipe. Meanwhile for $Re < 2100$ such turbulent puffs may spontaneously disappear, or for $Re \geq 2300$ they become destabilized either experiencing a splitting which results in higher number of puffs in the pipe or expanding its axial extension leading to long intermittent structures, the so-called *slugs* [5]. These expanding turbulent slugs result from an increase in the downstream front speed and thereby deviation from the upstream front speed. While the puff speed decreases, the downstream front speed in the slug range can increase [7]. The common understanding of this transition from puffs to slugs is a change from excitability to bistability. The works by Barkley et al. [7] provided deeper insight into front speeds in puffs and slugs, relaminarization statistics in a reduced model [8]. The nature of laminar-turbulent transition has been studied for more than a century. The recent review by Nikitin [9] provides a pretty detailed overview on this topic, based on theoretical, experimental, and numerical investigations of flows and turbulent structures in a round pipe at transition Reynolds numbers.

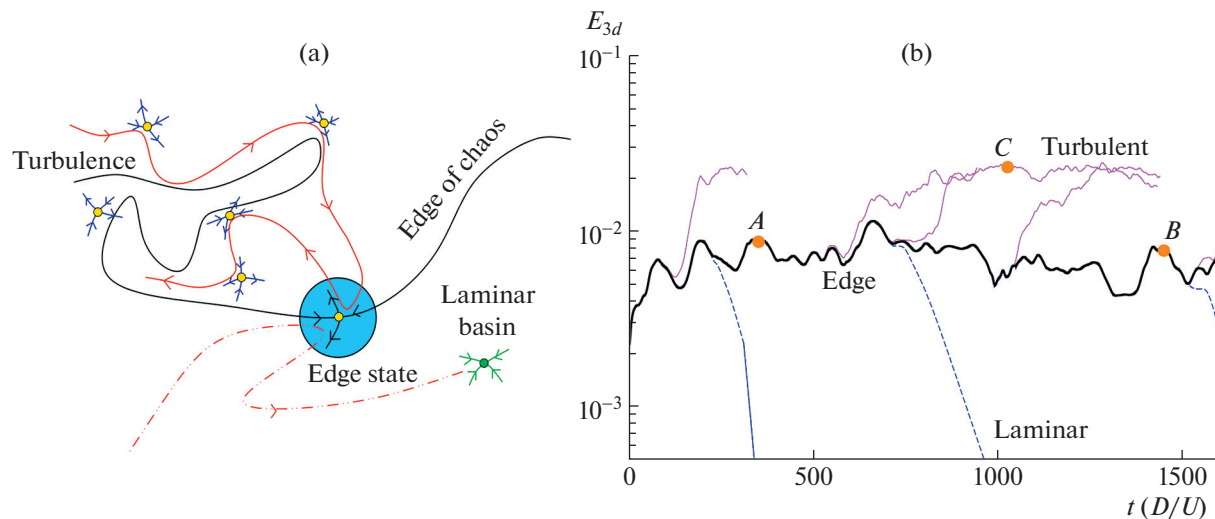


Fig. 1. (a) Schematic representation of the state space of transient turbulence in pipe flow. Laminar flow state is an attractor for which, with increasing Re , its basin of attraction reduces. The edge of chaos separates such trajectories which either relaminarise or become turbulent but at the same time is wrapped up into turbulent saddle [23, 35] allowing an unwinding route to the laminar state. (b) Dynamics of pipe flow around the edge for $Re = 2250$. Temporal evolution of the kinetic energy E_{3d} (of three-dimensional Fourier modes) is monitored. The thin magenta (solid) lines correspond to flow trajectories that become turbulent, whereas the blue (dashed) lines show trajectories that relaminarise. The thick solid line indicates the edge-trajectories that hang around the edge of chaos, i.e., they neither go turbulent nor relaminarise. A, B, and C indicate parameters for which snapshots of isosurfaces are presented in Fig. 3.

The dynamical system approaches suggest that invariant solutions of the Navier–Stokes equations, such as traveling waves (TWs) [10–12] and unstable periodic orbits in pipe flow, act as building blocks of the disordered and chaotic dynamics [13, 14]. Thus turbulence can be understood as a “walk-through” (Fig. 1a) of the field of invariant solutions [14, 15]. One most prevailing view is that a chaotic attractor may characterize turbulence whereby it is believed that one can construct its skeleton [16] from such invariant solutions of Navier–Stokes equations.

Identifying turbulent puffs as a structural unit of turbulence they can be understood as precursors of fully turbulent dynamics, which suggests them an interesting hydrodynamic object. But unfortunately their real dynamics is quite complex and uncertain, since the processes involved are stochastic, and the individual trajectories follow each other in a random manner. Therefore the main idea is to obtain some information from an analysis of simpler structures. Using edge-tracking techniques [13, 17–19] such solutions arise on a separatrix in the phase space between the both distinguishable domains of attraction, either the laminar and turbulent flow regimes. What kind of (relative) periodic orbit identifies the edge state may depend on the presence of certain spatial symmetries, e.g., TW for rotational or mirror + shift-reflect symmetry [10, 11, 20]. These edge states, having some qualitative properties of a turbulent puff, are time-periodic in the reference frame traveling along the pipe with a constant velocity. Their overall simpler structure makes it possible to perform a detailed investigation of the properties. It has been shown that such edge states not only appear between laminar and turbulent dynamics in pipe flow [20, 21] they also intermediate between them [22]. Chantry et al. [23] observed the edge not to be an independent dynamical structure, instead it is a part of a chaotic saddle, wrapped around turbulence-generating structures. Lozar et al. [24] confirmed the existence of the edge state in laboratory experiments and found that these states govern the dynamics during the decay of turbulence underlining its potential relevance for turbulence control. Further adapting the concept of the edge to the case of a spatially developing Blasius boundary layer, Beneitez et al. [25] reinterpreted the edge as a manifold dividing the state space between bypass transition and classical transition as two main types of boundary layer transition. Aside the edge plays a crucial role in designing optimal perturbations and control methods [26, 27].

However, as studies regarding turbulent dynamics are computationally expensive, various restrictions have been applied. First and most common is the use of short domains (short pipes), which results in the observations of various invariant solutions. The simplest are exact TWs [10–12, 20]. The common problem of these studies regarding TWs is the fact that numerical simulations extend spatially for only a few pipe diameters. Thus these solutions are incapable of explaining either large-scale intermittence or local-

ization phenomena. Aside these, the next level of complexity in the hierarchy of invariant solutions are modulated TWs and relative periodic orbits (RPOs) [28]. Being restricted to short domains, these studies lack the most important experimental observation of localization.

Sufficiently large domains allowing for such localization, which has been observed in TWs and RPOs, were also considered but at cost of higher symmetry restrictions. Most commonly diametral symmetry and π -periodicity were applied to limit the numerical costs and/or to make simulations feasible at all. Avila et al. [13] observed that under such restrictions solutions on the separatrix appear as RPOs having the form of structures localized in space with a time-periodic behavior in a co-moving frame of reference. This is an indication that they contain mechanisms that control the dynamics of turbulent solutions. The works by Nikitin and Pimanov [29, 30] present a detailed analysis of solutions on the separatrix with respect to the mechanisms responsible for their self-maintenance. They revealed the nonlinear mechanism of the onset of streamwise vortices to be responsible for sustainment of near-wall streaks. Worth to point out that that the relative simplicity of the solutions is only detected in the considered symmetry subspace, where solutions appear to be RPOs. Despite the fact that all these works provide the deeper insight in the flow dynamics, they miss the fact that in the real, full space the edge is found to be chaotic [21, 22, 31, 32].

This work is focused on this point. Avoiding such full space complexity [31, 32] we identify the solution set underlying the chaotic dynamics using a small/minimal set of symmetry restrictions (only reflection symmetry) to mirror the real world scenario as close as possible. The edge states, followed by edge tracking, presented here are asymptotic states that are located at the laminar-turbulent boundary.

1. NUMERICAL METHODS

The incompressible flow of a Newtonian fluid is described by Navier–Stokes equations, which can be rendered dimensionless. Here we use the following characteristic scales: the lengths are non-dimensionalized by $D/2$ and the velocities are non-dimensionalized by $2U$. Thus, we obtain

$$\partial_t \mathbf{u} + \mathbf{u} \cdot \nabla \mathbf{u} = -\nabla p + 1/\text{Re} \nabla^2 \mathbf{u}, \quad \nabla \cdot \mathbf{u} = 0. \quad (1.1)$$

The only governing parameter is the Reynolds number Re . The no-slip boundary condition enforces $\mathbf{u} = 0$ on the walls and we choose to impose periodic boundary conditions in the streamwise direction, such that localized structures in sufficiently long pipes are fully representative of the infinite domain case.

Numerical simulations are carried out by means of a hybrid spectral/finite-difference code [28, 33, 34] formulated in the cylindrical coordinates (r, θ, z) . The method ensures a constant mass flux through a pipe, whose axial periodicity we fix at $\Lambda = 40D$.

Unless otherwise stated, the dynamics are deliberately constrained to be reflectional symmetric with respect to the diametral plane in order to render the problem more tractable

$$\mathbf{S}: (u, v, w)(r, \theta, z, t) = (u, -v, w)(r, -\theta, z, t) \quad (1.2)$$

which inhibits rotations about the pipe axis, while u , v , and w are the velocities in the radial, azimuthal, and axial directions, respectively. No other symmetries are explicitly enforced but they may arise spontaneously during the simulations.

Sufficient convergence is secured by employing high spatial resolutions of up to $M = \pm 16$ Fourier modes in the azimuthal direction (for $\theta \in [0, \pi]$), $N = 64$ compact finite-difference points in the radial direction, and $K = \pm 17 \times \Lambda/D$ Fourier modes in the streamwise direction. This code and resolution provided in the past excellent quantitative agreement with experiments regarding very subtle turbulent puff properties such as lifetime statistics [19]. Transitional dynamics on the laminar-turbulent boundary were computed with a time evolution code (second-order predictor-corrector method with the time step $\Delta t = 0.0025$) and applying the edge-tracking refining technique [17, 21]. The procedure is as follows: applying a sufficiently strong localized disturbance to the laminar flow, which then evolves into a turbulent puff, gives the first initial condition $\mathbf{v}_{\text{puf},f}$. This preliminarily found turbulent solution $\mathbf{v}_{\text{puf},f}$ is then used in the iteration procedure of calculating the limiting solution on the separatrix. Therefrom the new initial conditions are obtained subsequently by rescaling the amplitude of this puff (with subtracted laminar parabolic flow): $\mathbf{v}_\alpha = \mathbf{v}_{\text{lam}} + \alpha(\mathbf{v}_{\text{puf},f} - \mathbf{v}_{\text{lam}})$, $\alpha \in (0, 1)$, where $\mathbf{v}_{\text{puf},f}$ and \mathbf{v}_{lam} are the velocity fields of the puff and the laminar flow, respectively.

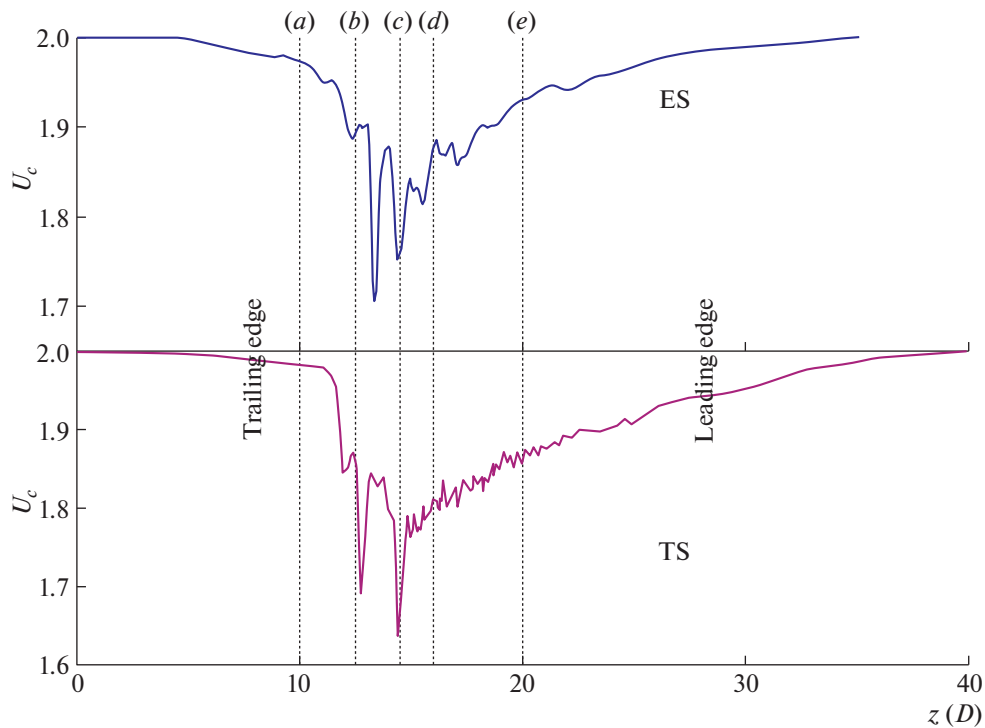


Fig. 2. Streamwise velocity U_c along the pipe centerline with a single structure present. Top: an edge state (ES). Bottom: a turbulent puff (TS) at $Re = 2250$. Flow is in the positive x direction, from left to right. Vertical lines with letters (a–e) indicate positions of cross sections presented in Fig. 4.

2. RESULTS

2.1. Edge States—Solutions on Separatrix

The edge-trajectory is bounded by two neighboring but qualitatively completely different trajectories, as one relaminarizes, while the other leads to turbulence. Figure 1b illustrates some trajectories including the edge (solid thick) and those which have either corresponding turbulent bounding (magenta thin lines) or relaminarizing (dashed blue lines) orbits for $Re = 2250$ and about 1600 time units. The edge-trajectory is obtained by applying the edge-tracking algorithm [13, 17, 31]. Worth mentioning that it is these noticeable differences in the corresponding energies of the edge and turbulent states that make it ultimately possible to track the edge trajectory with the shoot and bisection method [19, 21].

In contrast to higher symmetry restricted subspaces (e.g., including additional π -rotation symmetry) the edge trajectory does not show any sign to evolve into a kind of ordered, periodic or quasi-periodic oscillation, e.g., TWs [10, 11] or RPOs [13, 29, 36] (at least for times $t(D/U)$ up to 2000). Instead it does not settle on a simple invariant solution, which suggests that it remains chaotic, as also detected in the full space simulations [31]. This confirms the underlying structure of a strange saddle in the phase space. Which means that the here simplified simulations in reflection symmetric subspace came to the same result as it was detected in full space transition to turbulence in pipe flow [37]. Both support the conclusion that the dynamics in the edge does not settle down to a simple periodic or quasi-periodic state. In any case, the energy of edge trajectories remains well below turbulent levels (Fig. 1b) and therefore distinguishable.

2.1.1. Properties and characteristics of the edge state. Figure 2 illustrates the centerline velocities U_c for an edge state (ES) and a turbulent puff (TS) obtained by numerical simulation at $Re = 2250$ (flow from left to right). Consider the profile for TS (Fig. 2b): a sharp drop is present on the trailing edge/interface. This is a typical signature of puffs indicating sharp transition from laminar to turbulent flow. This clearly defined drop has been often used to determine the location of the puff. On the other side, at the leading edge/interface one observes a gradual increase in velocity corresponding to a slow recovery towards the laminar velocity.

Away from the localized puff, upstream and far downstream, the centerline velocity U_c approaches two times the bulk velocity U_B , which is the theoretical value for laminar flow. The gradual increase of the centerline velocity on the leading edge makes an exact length definition of the puff challenging. Immediately

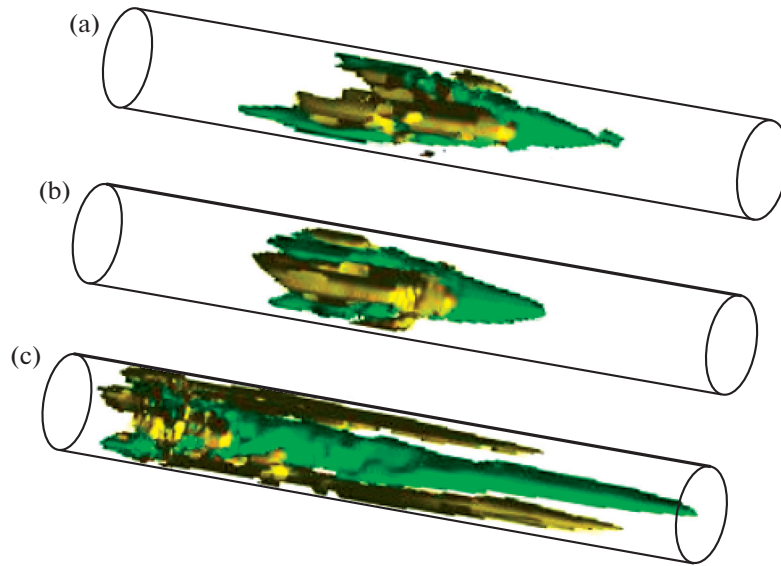


Fig. 3. Isosurfaces ($u_z = \pm 0.07$) of localized edge states (ES) at two moments of time (a, b) and a localized turbulent state (TS, puff) (c) (cf. points A, B, and C in Fig. 1) at $Re = 2250$. Green [yellow] indicates positive [negative] streamwise velocity. Flow direction from left to right. Only a central, $20D$ -long region of the pipe is shown.

after the sharp drop in U_c strong velocity fluctuations can be observed. Therein a region has been identified which shows the characteristics of fully developed turbulence [38].

The basic landmark of TS (Fig. 2, bottom) is shared by ES (Fig. 2, top), which demonstrates that the properties of localized turbulence can be captured by numerical solutions of Navier–Stokes equations found on the separatrix. However, there are differences. First of all, the increase in the velocity U_c (steeper slope) back to laminar flow ($U_c = 2$) is much faster for ES, which results in an overall shorter axial expansion, i.e., the length of ES (cf. Fig. 5). Secondly, the velocity fluctuations after the drop are less pronounced than in the corresponding puff. However, these fluctuations are clearly visible within the here used minimal set of symmetries in comparison to earlier works, which considered higher-order symmetries (π -rotation + reflection) (Fig. 2 in [13]) with the result that these fluctuations in ES basically disappear. Thus, the here detected dynamics are closer to the full space scenario.

2.1.2. Comparison of edge state vs puff. Figure 3 presents a qualitative comparison the ES at two moments of time on the separatrix (cf. Fig. 1) with a turbulent puff. The three-dimensional flow fields, illustrated as isosurfaces of the instantaneous axial velocity, show a qualitative agreement, although the ES structure remains simpler than that of TS at all times. The common feature of all structures is long regions of accelerated and decelerated motion close to the pipe wall. Both ES flow fields appear significantly less complex and show the higher spatial coherence than TS. Aside the smoother iso-surfaces, both the axial length of edge states and, in particular, that of the leading edge are significantly shorter than that of the turbulent puff. This results from the previously mentioned slow decrease in the axial velocity on the leading front and a sharper recovery on the trailing edge for TS. Meanwhile the edge state illustrates a moderate variation in its axial expansion, while maintaining its overall characteristics and shape, as a result of the chaotic behavior (cf. Fig. 1b) on the edge; (strong variation in streamwise velocity u_z and energy E in time). The trailing edge of the puff shows more complex dynamics with vortical structures that are tilted inside the volume and tear the streaks apart. The latter is one of the main reasons for the significant increase in energy within the turbulent puff compared to both ES (cf. Fig. 5a).

The instantaneous snapshots of cross-sectional velocity fields in the (r, θ) coordinates for ES and TS are presented in Fig. 4. The qualitative similarities between these states (axial positions are indicated by lines in Fig. 2) feature similar flow characteristics. ES (Fig. 4a) covers most of the dynamics of TS (Fig. 4b) within a generally smoother structure. The visible small-scale modulations in TS persist and reflect the intrinsically chaotic dynamics of the vortical structure (lines 2b and 2c). The smaller growth and more complex dynamics at the leading edge of TS can be visible in Fig. 4 (line 2e).

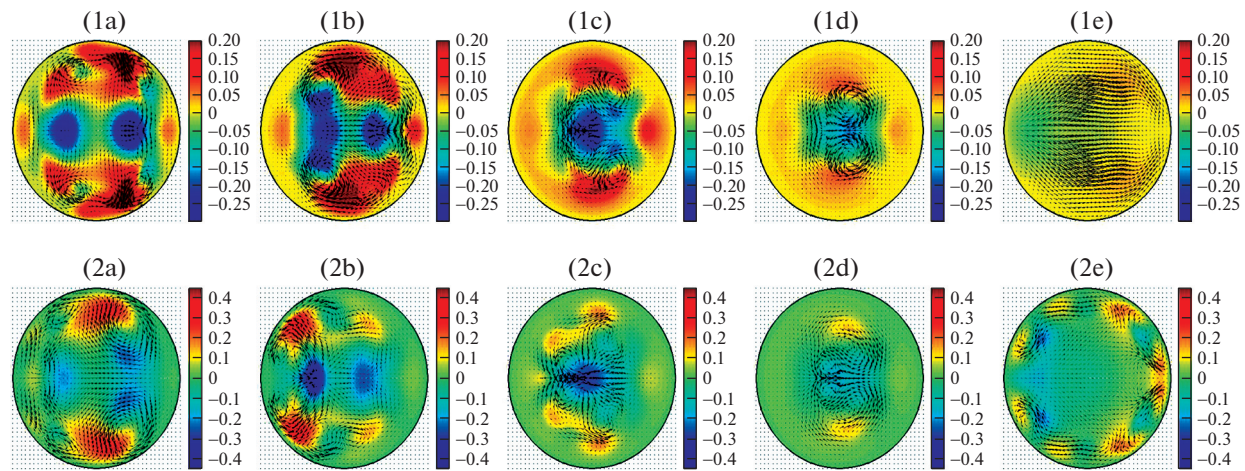


Fig. 4. Instantaneous snapshots of cross-sectional velocity fields in (r, θ) at different axial positions as indicated (cf. Fig. 2) for (1) edge state and (2) turbulent puff at $Re = 2250$. The in-plane velocity components are indicated by arrows, while the axial velocity is color-coded (blue for negative and red for positive). The laminar parabolic profile is subtracted. Color ranges from $-0.3U$ to $0.2U$. Maximum in-plane velocity is $-0.302U$. Red, yellow, and blue indicate the regions, where the streamwise flow speed is higher than, similar to, or lower than the corresponding parabolic profile.

2.2. Dependence on the Reynolds Number

We will now consider the case of higher Re for which the pipe turbulence changes and can split and/or appear in the form of growing slugs [5] instead of equilibrium puffs. Statistical properties are used to overcome the fact that all analyzed states are chaotic. Therefore averaged values over long time series ($t(D/U)$ about 1500 time units) are used instead of the properties at given time instants.

Figure 5a shows the axial distribution of the total modal kinetic energy E_{3d} of different edge states and the corresponding turbulent state for Re as indicated. The puff at $Re = 2250$ shows the typical energy distribution: on one side a large/wider extended leading edge (front), illustrated by a slow and mild exponential energy decay in the downstream region. On the other side a sharp trailing edge (rear), characterized by a fast exponential energy drop in the upstream region. Compared to TS, the corresponding edge state at the same $Re = 2250$ is obviously shorter. ES is basically characterized by extended interfaces in both leading and trailing edges. Moreover, the maximum energy and, particularly, the averaged energy are clearly lower for ES. With increasing Re the basic shape of ES remains the same with a slight axial expansion of the peak energy region. At the same time, the energy in the leading edge decreases slower moving toward the typical shape of a turbulent puff. Meanwhile, with increasing Re the maximum values in $E(z)$ for ES remain basically at the same level, while the minima slightly increase.

Figure 5b illustrates the variation with Re of the time-averaged energies corresponding to the edge and turbulent states, asymptotically approached by the edge and turbulent trajectories (cf. Fig. 1). The edge state energy does not show any noticeable variation within the explored Re range. The turbulent energy level is not only higher for all Re , compared to the one associated to the edge, it also continuously increases with greater Re . Moreover, the energy of the turbulent regime experiences a noticeable increase between $Re = 2400$ and $Re = 2500$. This is the result of the unbounded growth of the turbulent structures into a slug in this regime, which ultimately fill the entire domain. This can be notified in Fig. 5c illustrating the axial length l_z of the structures. Here l_z is chosen as the minimal axial extent containing 98% of the energy component (Fig. 5a). For $Re \geq 2500$ the turbulent structures fill the entire domain ($40D$).

SUMMARY

It is shown that numerical solutions of Navier–Stokes equations with a minimal set of (artificial) symmetry restrictions (here only reflection symmetry) allow to cover the key characteristics of the flow dynamics in the transitional regime toward turbulence in pipe flows. In order to determine this transition threshold in terms of the perturbation amplitude we investigate the edge of chaos/separatrix which divides the perturbations decaying toward the laminar flow from those which eventually trigger turbulence. The discovered edge states share the structural properties and the spatial complexity with turbulent puffs. Moreover, the separatrix appears to be chaotic, as it has been detected in full space simulations. This is an

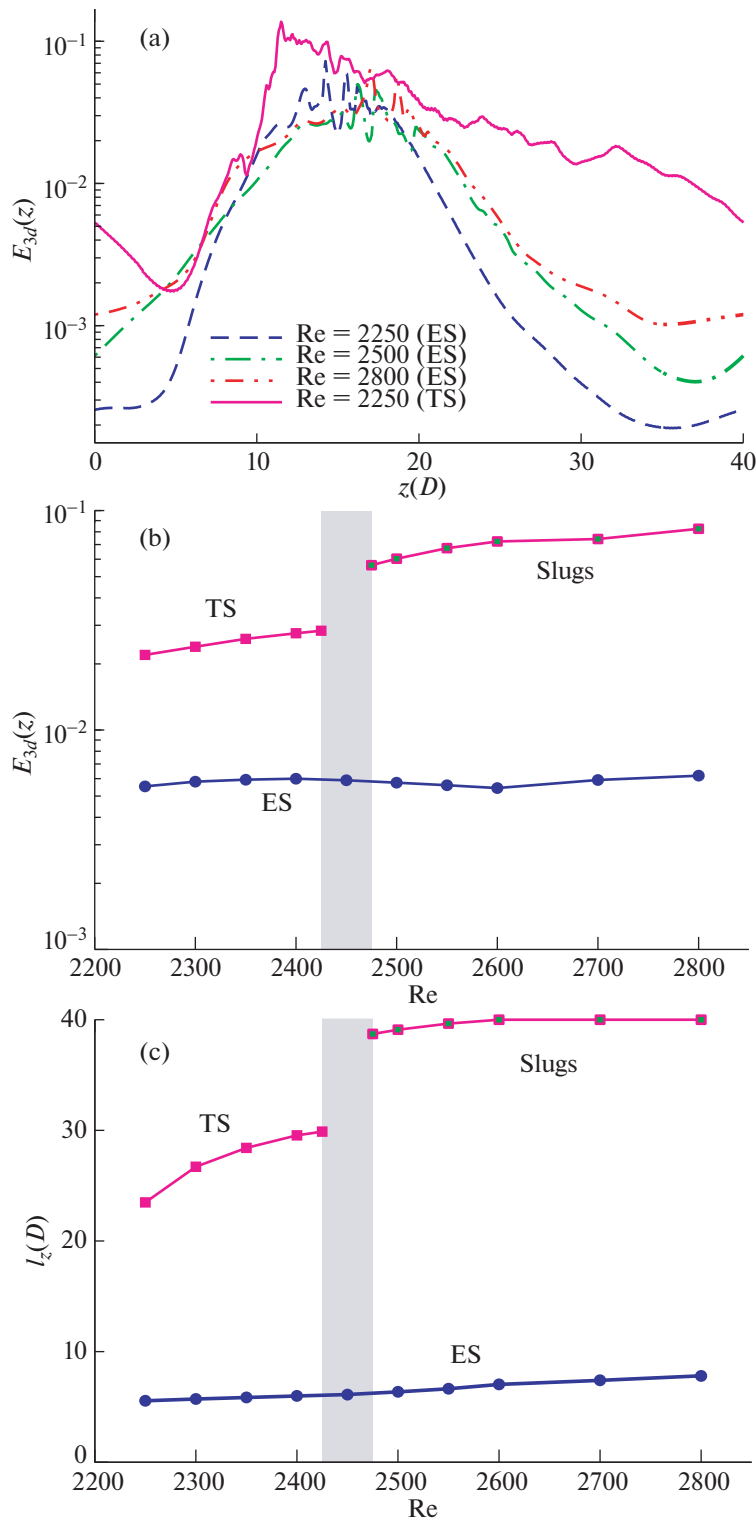


Fig. 5. Statistical properties of ESs and TSs as functions of Re. (a) Energy E_{3d} based on the axial position z and measured in the units of the radius. (b) Time-averaged energy E_{3d} . (c) Axial length l_z of ESs and TSs within the explored Re range.

important observation as it clearly overcomes the key problematic in subspaces with higher symmetry restrictions, e.g. the diametral symmetry and π -periodicity [13, 29, 30], where the separatrix is found to be time- (quasi-) periodic. To our knowledge, it is the first time that solutions with only reflection symmetry has been reported in pipe flow. The here detected solutions turn out to be similarly complex as solu-

tions without additional restrictions. Although this observation may provide only few new opportunities for analysis in comparison with the full space solutions, it clearly highlights the importance of awareness of the respective subspace, which may strongly change and/or simplify the dynamics.

The here presented results under reflection symmetry are in good agreement with previously reported localized edge states in pipe flows with no symmetry [31] and therefore provide a great first step to get an easy and fast idea of the dynamics before using economic and time-expensive simulations. Within the here studied transitional regime $Re \in [2200, 2800]$ the edge states can provide more insight into the transition to turbulent dynamics than the study of already fully turbulent states in pipe flows. Aside, with increasing Re an expansion of turbulent puffs into slugs and therefore the loss of localization becomes crucial. Here, greater domains and, together with this, higher computational efforts are necessary to capture these processes. Clearly, future work is required, but knowing about the similarity of the flow dynamics and structures obtained in the reflection symmetry subspace and the full space can surely help with respect to one of the main challenging problems regarding the study of turbulent motion. Such simulations are typically highly numerically expensive in both the computation time and the computation power.

FUNDING

Sebastian Altmeyer is a Serra Húnter Fellow. This work was supported by the Spanish Government grant no. PID2019-105162RB-I00.

CONFLICT OF INTEREST

The authors declares that he has no conflicts of interest.

REFERENCES

1. Meseguer, A. and Trefeten, L.N., Linearized pipe flow to Reynolds number 10^7 , *J. Comput. Phys.*, 2003, vol. 186, p. 178.
2. Reynolds, O., An experimental investigation of the circumstances which determine whether the motion of water shall be direct or sinuous, and of the law of resistance in parallel channels, *Phil. Trans. Roy. Soc. London. A*, 1883, vol. 174, p. 935.
3. Hof, B., Juel, A., and Mullin, T., Scaling of the threshold of pipe flow turbulence, *Phys. Rev. Lett.*, 2003, vol. 91, p. 244502.
4. Peixinho, J. and Mullin, T., Decay of turbulence in pipe flow, *Phys. Rev. Lett.*, 2006, vol. 96, p. 094501.
5. Wygnanski, I.J. and Champagne, F.H., On transition in a pipe. Part 1. The origin of puffs and slugs and the flow in a turbulent slug, *J. Fluid Mech.*, 1973, vol. 59, p. 281.
6. Wygnanski, I., Sokolov, J.M., and Friedman D., On transition in a pipe. Part 2. The equilibrium puff, *J. Fluid Mech.*, 1975, vol. 69, p. 283.
7. Barkley, D., Song, B., Mukund, V., Lemoult, G., Avila, M., and Hof, B., The rise of fully turbulent flow, *Nature*, 2015, vol. 526, pp. 550–553.
8. Willis, A.P. and Kerswell, R.R., Turbulent dynamics of pipe flow captured in a reduced model: puff relaminarization and localized “edge” states, *J. Fluid Mech.*, 2009, vol. 619, pp. 213–233.
9. Nikitin, N.V., Transition problem and localized turbulent structures in pipes, *Fluid Dyn.*, 2021, vol. 56, no. 1, pp. 31–44.
10. Faisst, H. and Eckhardt, B., Traveling waves in pipe flow, *Phys. Rev. Lett.*, 2003, vol. 91, p. 224502.
11. Pringle, C.C.T. and Kerswell, R.R., Asymmetric, helical, and mirror-symmetric traveling waves in pipe flow, *Phys. Rev. Lett.*, 2007, vol. 99, p. 074502.
12. Mellibovsky, F. and Meseguer, A., Critical threshold in pipe flow transition, *Phil. Trans. Roy. Soc. London. A*, 2009, vol. 367, p. 545.
13. Avila, M., Mellibovsky, F., Roland, N., and Hof, B., Streamwise-localized solutions at the onset of turbulence in pipe flow, *Phys. Rev. Lett.*, 2013, vol. 110, p. 224502.
14. Hof, B., van Doorne, C.W.H., Westerweel, J., Nieuwstadt, F.T.M., Faisst, H., Eckhardt, B., Wedin, H., Kerswell, R.R., and Waleffe, F., Experimental observation of nonlinear traveling waves in turbulent pipe flow, *Science*, 2004, vol. 305, p. 1594.
15. Hof, B., de Lozar, A., Kuik, D.J., and Westerweel, J., Repeller or attractor? Selecting the dynamical model for the onset of turbulence in pipe flow, *Phys. Rev. Lett.*, 2008, vol. 101, p. 214501.
16. Gibson, J.F., Halcrow, J., and Cvitanovi'c, P., Visualizing the geometry of state space in plane Couette flow, *J. Fluid Mech.*, 2008, vol. 611, pp. 107–130.

17. Itano, T. and Toh, S., The dynamics of bursting process in wall turbulence, *J. Phys. Soc. Japan*, 2001, vol. 70, pp. 703–716.
18. Skufca, J.D., Yorke, J.A., and Eckhardt, B., Edge of chaos in a parallel shear flow, *Phys. Rev. Lett.*, 2013, vol. 96, p. 174101.
19. Avila, M., Willis, A.P., and Hof, B., On the transient nature of localized pipe flow turbulence, *J. Fluid Mech.*, 2010, vol. 646, p. 127.
20. Duguet, Y., Willis, A.P., and Kerswell, R.R., Transition in pipe flow: the saddle structure on the boundary of turbulence, *J. Fluid Mech.*, 2008, vol. 613, pp. 255–274.
21. Schneider, T.M., Eckhardt, B., and Yorke, J.A., Turbulence transition and the edge of chaos in pipe flow, *Phys. Rev. Lett.*, 2007, vol. 99, p. 034502.
22. Schneider, T.M. and Eckhardt, B., Edge states intermediate between laminar and turbulent dynamics in pipe flow, *Phil. Trans. Roy. Soc. London. A*, 2008, vol. 367, pp. 577–587.
23. Chantry, M. and Schneider, T.M., Studying edge geometry in transiently turbulent shear flows, *J. Fluid Mech.* 2014, vol. 747, pp. 506–517.
24. De Lozar, A., Mellibovsky, F., Avila, M., and Hof, B., Edge state in pipe flow experiments, *Phys. Rev. Lett.*, 2012, vol. 108, p. 214502.
25. Beneitez, M., Duguet, Y., Schlatter, P., and Henningson, D.S., Edge tracking in spatially developing boundary layer flows, *J. Fluid Mech.*, 2019, vol. 881, pp. 164–181.
26. Kerswell, R.R., Nonlinear nonmodal stability theory, *Annu. Rev. Fluid Mech.*, 2018, vol. 50, pp. 319–345.
27. Rabin, S.M.E., Caulfield, C.P., and Kerswell, R.R., Triggering turbulence efficiently in plane Couette flow, *J. Fluid Mech.*, 2012, vol. 712, pp. 244–272.
28. Willis, A.P., Cvitanovi'c, P., and Avila, M., Revealing the state space of turbulent pipe flow by symmetry reduction, *J. Fluid Mech.*, 2013, vol. 721, p. 514.
29. Nikitin, N.V. and Pimanov, V.O., Numerical study of localized turbulent structures in a pipe, *Fluid Dyn.*, 2015, vol. 50, no. 5, pp. 655–664.
30. Nikitin, N.V. and Pimanov, V.O., Sustainment of oscillations in localized turbulent structures in pipes, *Fluid Dyn.*, 2018, vol. 53, no. 1, pp. 65–73.
31. Mellibovsky, F., Meseguer, A., Schneider, T., and Eckhardt, B., Transition in localized pipe flow turbulence, *Phys. Rev. Lett.*, 2009, vol. 103, p. 054502.
32. Avila, K., Moxey, D., de Lozar, A., Avila, M., Barkley, D., and Hof, B., The onset of turbulence in pipe flow, *Science*, 2011, vol. 333, p. 192.
33. Willis, A.P. and Kerswell, R.R., Turbulent dynamics of pipe flow captured in a reduced model: puff relaminarization and localized “edge” states, *J. Fluid Mech.*, 2009, vol. 619, p. 213.
34. Willis, A.P., The Openpipeflow Navier–Stokes solver, *SoftwareX*, 2017, vol. 6, pp. 124–127.
35. Lebovitz, N.R., Boundary collapse in models of shear-flow transition, *Commun. Nonlinear Sci. Numer. Simul.*, 2012, vol. 17, no. 5, pp. 2095–2100.
36. Chantry, M., Willis, A.P., and Kerswell, R.R., Genesis of streamwise-localized solutions from globally periodic traveling waves in pipe flow, *Phys. Rev. Lett.*, 2014, vol. 112, p. 164501.
37. Eckhard, B., Turbulence transition in pipe flow: some open questions, *Nonlinearity*, 2007, vol. 21, no. 1, pp. 1–11.
38. Bandyopadhyay, P.R., Aspects of the equilibrium puff in transitional pipe-flow, *J. Fluid Mech.*, 1986, vol. 163, p. 439.